EVALUATION OF CURRENT NONLINEAR STATIC PROCEDURES FOR CONCRETE BUILDINGS USING RECORDED STRONG-MOTION DATA

Rakesh K. Goel and Charles Chadwell

Department of Civil and Environmental Engineering
California Polytechnic State University, San Luis Obispo

Abstract

This paper evaluates current Nonlinear Static Procedures (NSPs) specified in the FEMA-356, ASCE-41, ATC-40, and FEMA-440 documents using strong-motion data from reinforced-concrete buildings. For this purpose, peak roof (or target node) displacements estimated from the NSPs are compared with the value derived from recorded motions. It is shown that: (1) the NSPs either overestimate or underestimate the peak roof displacement for several of the buildings considered in this investigation; (2) the ASCE-41 Coefficient Method (CM), which is based on recent improvements to the FEMA-356 CM suggested in FEMA-440 document, does not necessarily provide better estimate of roof displacement; and (3) the improved FEMA-440 Capacity Spectrum Method (CSM) generally provides better estimates of peak roof displacements compared to the ATC-40 CSM. However, there is no conclusive evidence of either the CM procedures (FEMA-356 or ASCE-41) or the CSM procedure (ATC-40 or FEMA-440) leading to better estimate of the peak roof displacement when compared with the value derived from recorded motions.

Introduction

Estimating seismic demands at low performance levels, such as life safety and collapse prevention, requires explicit consideration of inelastic behavior of the structure. While nonlinear response history analysis (RHA) is the most rigorous procedure to compute seismic demands, current structural engineering practice prefers to use the nonlinear static procedure (NSP) or pushover analysis. The two key steps in estimating seismic demands in NSP are: (1) estimation of the target node displacement; and (2) pushover analysis of the structure subjected to monotonically increasing lateral forces with specified height-wise distribution until the target displacement is reached. Both the force distribution and target displacement are typically based on the assumption that the response is controlled by the fundamental mode and that the mode shape remains unchanged after the structure yields.

The two widely used procedures to estimate the target displacement are: (1) the Coefficient Method (CM) defined in the FEMA-356 document (ASCE, 2000); and (2) the Capacity Spectrum Method (CSM) specified in ATC-40 document (ATC-40, 1997). The CM utilizes a displacement modification procedure in which several empirically derived factors are used to modify the response of a linearly-elastic, single-degree-of-freedom (SDOF) model of the structure. The CSM is a form of equivalent linearization. This technique uses empirically derived relationships for the effective period and damping as a function of ductility to estimate the response of an equivalent linear SDOF oscillator.

Various researchers have found that the CM and CSM may provide substantially different estimates of target displacement for the same ground motion and the same building (Aschheim et al., 1998; Akkar and Metin, 2007; Chopra and Goel, 2000; Goel, 2007; Miranda and Ruiz-Garcia, 2002) and have proposed improved procedures for estimating the target displacement. The ATC-55 project, which led to publication of the FEMA-440 document (ATC-55, 2003), undertook a comprehensive examination of the existing research in this area and has proposed improvements to both the CM and CSM.

Most previous investigations on development and evaluation of NSPs are based on numerical modeling studies; a comprehensive list of previous investigations is available in the FEMA-440 document (ATC-55, 2003). Recorded motions of strongly shaken buildings, especially those deformed into the inelastic range, provide a unique opportunity to evaluate such procedures. Therefore, the principal objective of this investigation is to evaluate the current NSPs for seismic analysis and evaluation of building structures using strong-motion records of reinforced-concrete buildings. The NSPs to be evaluated are: (1) Coefficient Method in the FEMA-356 document; (2) Capacity Spectrum Method in the ATC-40 report; and (3) improved Coefficient Method in ASCE-41 document; and (4) improved Capacity Spectrum Method proposed in the FEMA-440 document. The accuracy of these NSPs is evaluated by comparing the peak roof (or target node) displacement computed from various NSPs with that derived directly from recorded motions.

Selected Buildings and Strong-Motion Data

Recorded motions of buildings that were strongly shaken and potentially deformed beyond the yield limit during the earthquake are required for this investigation. For this purpose, five concrete buildings, ranging from low-rise to high-rise, have been selected (Table 1). The strong-motion data used in this investigation are also identified in Table 1 for each building. These data are available from the US National Center for Engineering Strong Motion Data (NCESMD) (http://www.strongmotioncenter.org). Following is a brief description of each of the five selected buildings.

Table 1. Five concrete buildings selected.

Buildings name	CSMIP Station	Number of Stories	Strong-Motion Data from
Imperial County Services Building, El Centro	01260	6/0	1979 Imperial Valley Earthquake
13-Story Commercial Building, Sherman Oaks	24322	13/2	1994 Northridge Earthquake
20-Story Hotel, North Hollywood	24464	20/1	1994 Northridge Earthquake
4-Story Commercial Building, Watsonville	47459	4/0	1989 Loma Prieta Earthquake
3-Story UCSB Office Building, Santa Barbara	25213	3/0	1978 Santa Barbara Earthquake

6-Story Imperial County Services Building in El Centro

This building has open first story and five occupied stories (Figure 1). Designed in 1968, its vertical load carrying system consists of 12.7 cm (5 inch) reinforced-concrete (RC) thick slabs supported by RC pan joists spanning in transverse direction which in turn are supported by RC frame spanning in the longitudinal direction. The lateral load system consists of RC shear walls in the transverse direction and moment resisting frames in the longitudinal direction. The shear walls are offset in the first story compared to upper stories. The foundation system consists of piles under each column with pile caps connected with RC beams.

The Imperial County Services building was instrumented in 1976 with 13 sensors at four levels of the building and 3 sensors at a reference free-field site. The sensors in the building measure horizontal accelerations at ground floor, 2nd floor, 4th floor, and roof; and vertical acceleration at ground floor (Figure 1). The recorded motions of this building are available only for the 1979 Imperial Valley earthquake, during which this building was damaged and subsequently demolished. The peak recorded accelerations during this earthquake were 0.34g at the ground floor and 0.58g at the roof level.

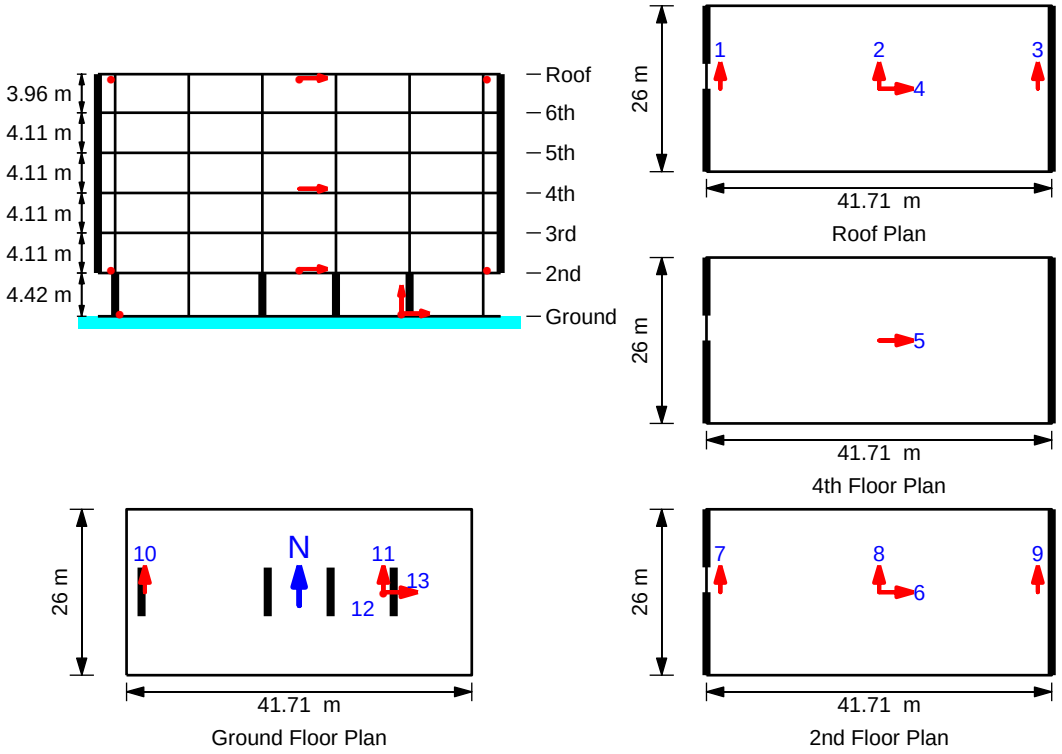

Figure 1. Imperial County Services Building.

13-Story Commercial Building in Sherman Oaks

This building has 13 stories above and two floors below the ground (Figure 2). Designed in 1964, its vertical load carrying system consists of 11.4 cm (4.5 inch) thick slabs supported by concrete beams, girders, and columns. The lateral load system consists of moment resisting

concrete frames in the upper stories and concrete shear walls in the basements. The foundation system consists of concrete piles.

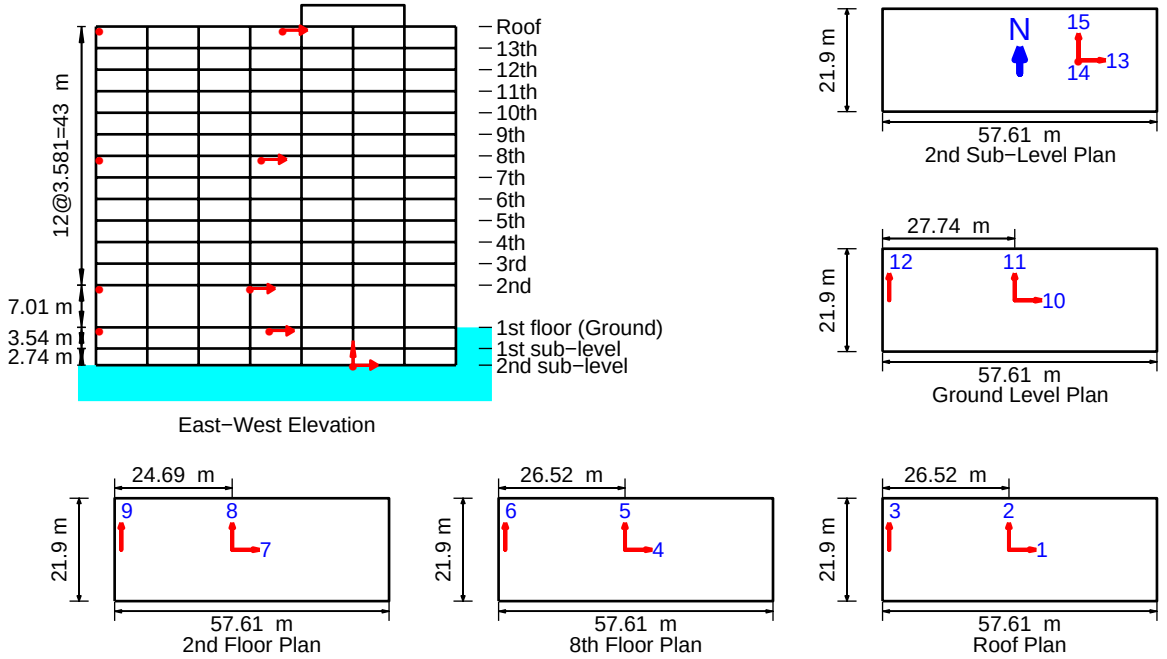

Figure 2. 13-Story Commercial Building in Sherman Oaks.

This building was instrumented in 1977 with 15 sensors on five levels of the building. The sensors in the building measure horizontal accelerations at the 2nd sub-basement level, ground level, 2nd floor, 8th floor, and roof level; and vertical accelerations at the 2nd sub-basement (Figure 2). Although this building yielded recorded motions during four major earthquakes – 1994 Northridge, 1992 Landers, 1991 Sierra Madre, and 1987 Whittier – the strongest shaking occurred during the 1994 Northridge earthquake when peak recorded accelerations were 0.46g at the basement and 0.65g in the structure. The strong-motion data from this earthquake has been used in this investigation. The building is reported to have suffered cracks at many beam-column joints during the 1994 Northridge earthquake (Shakal et al., 1994) and has subsequently been strengthened with friction dampers.

20-Story Hotel in North Hollywood

This building has 20 stories above and one floor below the ground (Figure 3). Designed in 1966, its vertical load carrying system consists of 11.4 cm (4.5 inch) to 15 cm (6 inch) thick RC slabs supported by concrete beams and columns. The lateral load system consists of ductile moment resisting concrete frames in both directions. The foundation system consists of spread footing below columns.

This building was instrumented in 1983 with 16 sensors on five levels of the building. The sensors in the building measure horizontal accelerations at the basement level, 3rd floor, 9th floor, 16th floor, and roof level; and vertical acceleration at the basement (Figure 3). Although this building yielded recorded motions during three major earthquakes – 1994 Northridge, 1991

Sierra Madre, and 1987 Whittier – the strongest shaking occurred during the 1994 Northridge earthquake when peak recorded accelerations were 0.33g at the basement and 0.66g in the structure. The data from 1994 Northridge earthquake has been used in this investigation.

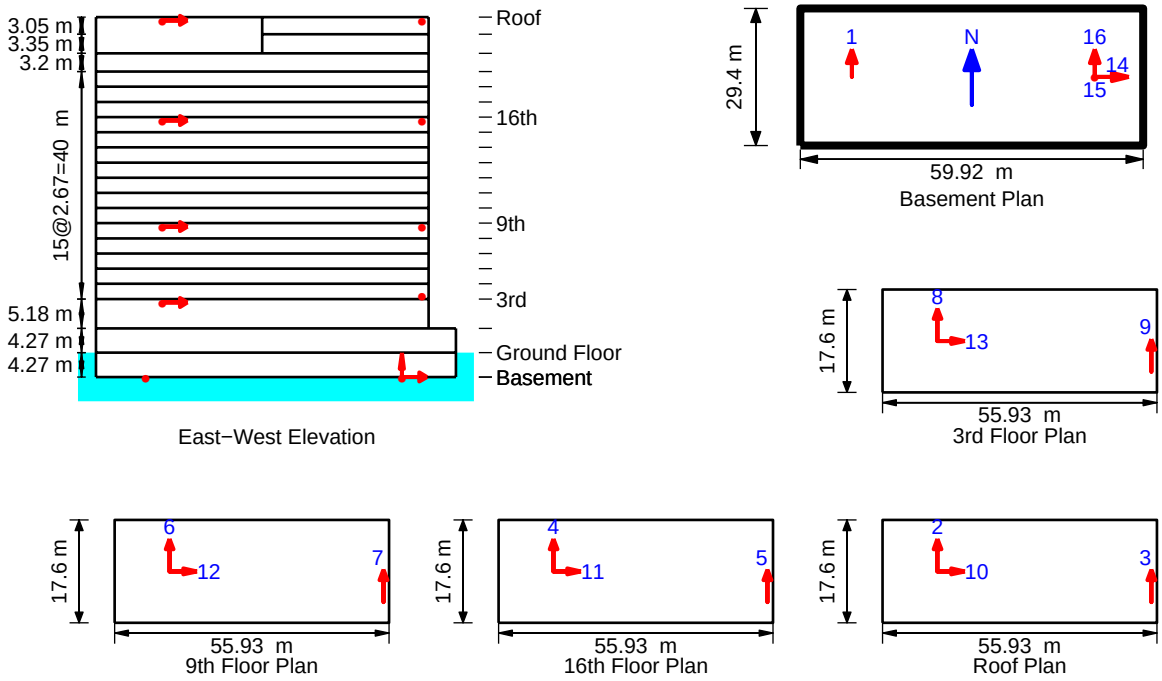

Figure 3. 20-Story Hotel in North Hollywood.

4-Story Commercial Building in Watsonville

This commercial building has 4 stories above the ground (Figure 4). Originally designed and constructed in 1948 as a three-story building, the fourth story was added in 1955. Its vertical load carrying system consists of concrete slabs supported by composite concrete-steel columns. The lateral load system consists of concrete shear walls in both directions. The foundation system consists of spread footing below shear walls.

This building was instrumented in 1982 with 13 sensors on three levels of the building. The sensors in the building measure horizontal accelerations at the ground floor, 3rd floor, and roof level; and vertical accelerations at four corners of the building at the ground floor (Figure 4). This building yielded recorded motions during 1989 Loma Prieta earthquake with peak accelerations of 0.66g at the ground level and 1.24g in the structure.

3-Story UCSB Office Building in Santa Barbara

This office building on the campus of University of California at Santa Barbara has 3 stories above the ground (Figure 5). Originally designed and constructed in 1960, this building was strengthened in 1975 with shear walls in both directions. The vertical load carrying system of the original building consists of concrete slabs supported by joists and RC/masonry columns. The lateral load system of the strengthened building now consists of concrete shear walls in both

directions. The foundation system consists of caissons under columns with tie beams and 10 cm (4 inch) thick slab.

This building was instrumented in 1975 with 9 sensors on three levels of the building, and 3 sensors at a reference free-field site. The sensors in the building measure horizontal accelerations at the ground floor, 3rd floor, and roof level; and vertical acceleration at the ground floor (Figure 5). This building yielded recorded motions during 1978 Santa Barbara earthquake with peak accelerations of 0.4g at the ground level and 1g in the structure.

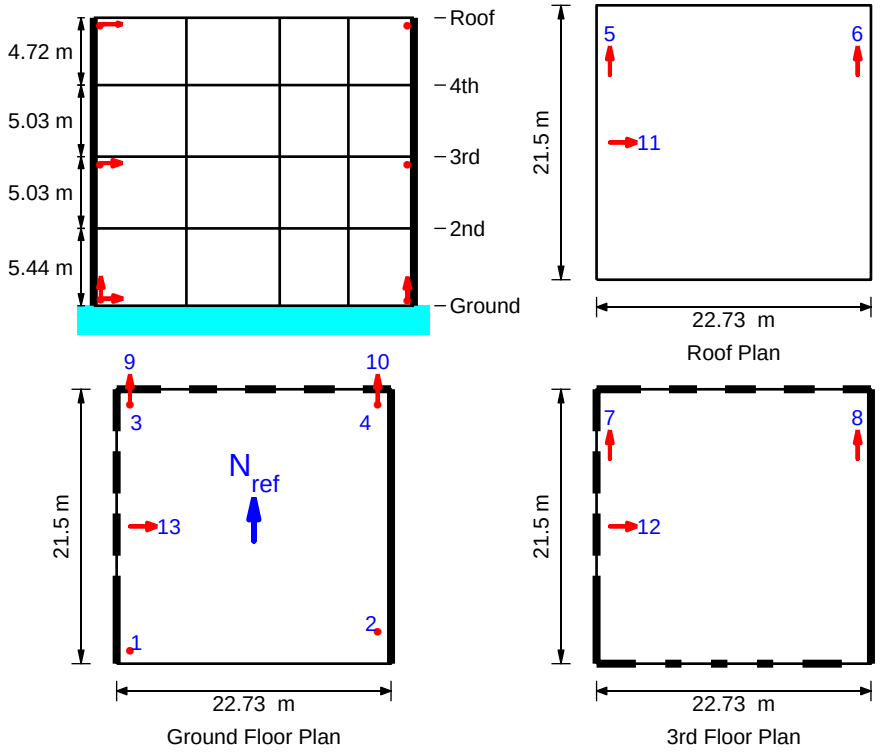

Figure 4. 4-Story Commercial Building in Watsonville.

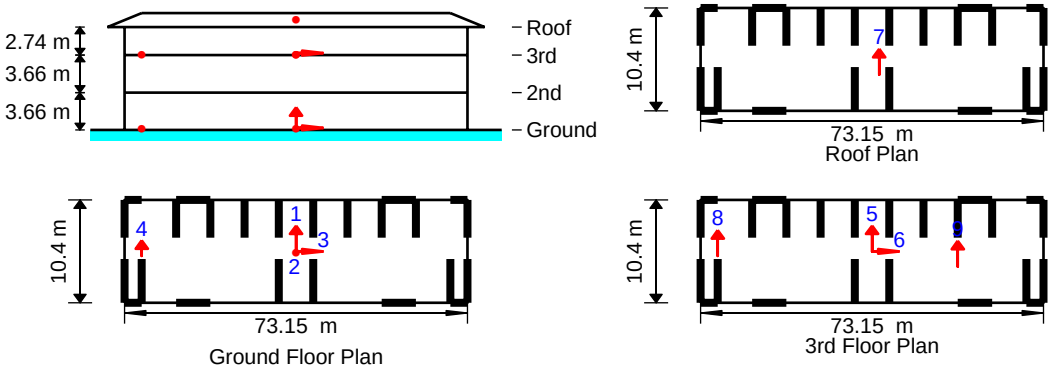

Figure 5. 3-Story Office Building in Santa Barbara.

Current Nonlinear Static Procedures (NSPs)

NSPs in the FEMA-356, ATC-40, FEMA-440, and ASCE-41 documents require development of a pushover curve which is defined as the relationship between the base shear and lateral displacement of a control node. The height-wise distributions of lateral loads for pushover analysis is typically selected from: (1) Equivalent lateral force (ELF) distribution: $s_j^* = m_j h_j^k$ (the floor number $j = 1, 2 \ldots N$) where s_j^* is the lateral force and m_j the mass at jth floor, h_j is the height of the jth floor above the base, and the exponent $k = 1$ for fundament period $T_1 \le 0.5 \sec$, $k = 2$ for $T_1 \ge 2.5 \sec$; and varies linearly in between; (2) Fundamental mode distribution: $s_j^* = m_j \phi_{j1}$ where ϕ_{j1} is the fundamental mode shape component at the jth floor; and (3) Response Spectrum Analysis (RSA) distribution: the vector of lateral forces $\mathbf{s}^*$ is defined by the lateral forces back-calculated from the story shears determined by linear response spectrum analysis of the structure including sufficient number of modes to capture 90% of the total mass; and (4) "Uniform" distribution: $s_j^* = m_j$ in which m_j is the mass and s_j^* is the lateral force at jth floor. The FEMA-356 NSP requires development of the pushover curve for two height-wise distributions of lateral forces: one selected from the first three of the aforementioned distributions and the second selected as the "Uniform" distribution. The ATC-40, FEMA-440, and ASCE-41 NSP require development of the pushover curve only for the fundamental mode distribution.

The structure is pushed statically to a target displacement at the control node to check for the acceptable structural performance. The NSP in the FEMA-356, FEMA-440, ATC-40, and ASCE-41 documents differ primarily in computation of this target displacement. These methods are summarized next.

FEMA-356 Coefficient Method

The target displacement in the Coefficient Method (CM), specified in the FEMA-356 document is computed from

$$\delta_t = C_0 C_1 C_2 C_3 S_a \frac{T_e^2}{4\pi^2} g \tag{1}$$

where S_a = Response spectrum acceleration at the effective fundamental vibration period and damping ratio of the building under consideration; g = Acceleration due to gravity; T_e = Effective fundamental period of the building in the direction under consideration computed by modifying the fundamental vibration period from elastic dynamic analysis, e.g., eigen-value analysis, T_i, by:

$$T_e = T_i \sqrt{\frac{K_i}{K_e}} \tag{2}$$

in which K_i is the elastic stiffness of the building and K_e is the effective stiffness of the building obtained by idealizing the pushover curve as a bilinear relationship; C_0 = Modification factor that relates the elastic response of a Single-Degree-of-Freedom (SDF) system to the elastic displacement of the Multi-Degree-of-Freedom (MDF) building at the control node taken as the first mode participation factor or selected from tabulated values in FEMA-356; C_1 = Modification factor that relates the maximum inelastic and elastic displacement of the SDF system computed from

$$C_1 = \begin{cases} 1.0; & T_e \geq T_s \\ \dfrac{1.0 + (R-1)T_s/T_e}{R}; & T_e < T_s \\ 1.5; & T_e < 0.1s \end{cases} \tag{3}$$

in which R is the ratio of elastic and yield strengths and T_s is the corner period where the response spectrum transitions from constant pseudo-acceleration to constant pseudo-velocity; C_2 = Modification factor to represent the effects of pinched hysteretic shape, stiffness degradation, and strength deterioration selected either from tabulated values depending on the framing system (see FEMA-356 for details of various framing systems) and the performance level or taken as one for nonlinear analysis; and C_3 = Modification factor to represent increased displacement due to P-delta effects computed from

$$C_3 = \begin{cases} 1.0; & \alpha \geq 0 \\ 1.0 + \dfrac{|\alpha|(R-1)^{3/2}}{T_e}; & \alpha < 0 \end{cases} \tag{4}$$

in which α is the ratio of the post-yield stiffness to effective elastic stiffness.

ATC-40 Capacity Spectrum Method

The target displacement in the Capacity Spectrum Method (CSM) specified in the ATC-40 document is computed as the maximum displacement of a linearly-elastic SDF system with equivalent period, T_{eq}, and equivalent damping ratio, ζ_{eq} given by:

$$T_{eq} = T_o\sqrt{\frac{\mu}{1+\alpha\mu-\alpha}};\ \zeta_{eq} = \zeta_o + \kappa\frac{1}{\pi}\frac{(\mu-1)(1-\alpha)}{\mu(1+\alpha\mu-\alpha)} \tag{5}$$

in which T_o is the initial period of vibration of the nonlinear system, α is the post-yield stiffness ratio, μ is the maximum displacement ductility ratio, and κ is the adjustment factor to approximately account for changes in hysteretic behavior of reinforced concrete structure. The ATC-40 document defines three types of hysteretic behaviors – Type A with stable, reasonably full hysteretic loops; Type C with severely pinched and/or degraded loops; and Type B between

Types A and C – and provides equations for computing κ for each of the three types of hysteretic behavior.

Since the equivalent linearization procedure requires prior knowledge of the displacement ductility ratio (see Eq. 5), ATC-40 document describes three iterative procedures: Procedures A, B, and C. Procedures A and B are the most transparent and convenient for programming, whereas Procedure C is purely a graphical method that is not suitable for programming. Details of these procedures are available in ATC-40 document and are not presented here for brevity.

ASCE-41 Coefficient Method

The ASCE-41 CM is based on the improvements to the FEMA-356 CM (Eq. 1) proposed in the FEMA-440 document. In the ASCE-41 CM, the coefficient C_1 is given by

$$C_1 = \begin{cases} 1.0; & T_e > 1.0\,\text{s} \\ 1.0 + \dfrac{R-1}{aT_e^2}; & 0.2\,\text{s} < T_e \le 1.0\,\text{s} \\ 1.0 + \dfrac{R-1}{0.04a}; & T_e \le 0.2\,\text{s} \end{cases} \tag{6}$$

in which a is equal to 130 for site class A and B, 90 for site class C, and 60 for site classes D, E, and F (see ASCE-41 for details of various site classes), respectively. The coefficient C_2 is given by

$$C_2 = \begin{cases} 1.0; & T_e > 0.7\,\text{s} \\ 1 + \dfrac{1}{800}\left(\dfrac{R-1}{T_e}\right)^2; & T_e \le 0.7\,\text{s} \end{cases} \tag{7}$$

Finally, ASCE-41 CM has dropped the coefficient C_3 but imposes a limitation on strength to avoid dynamic instability. This limitation on strength is specified by imposing a maximum limit on R given by

$$R_{\max} = \frac{\Delta_d}{\Delta_y} + \frac{|\alpha_e|^{-h}}{4}; \quad h = 1.0 + 0.15\ln(T_e) \tag{8}$$

in which Δ_d is the deformation corresponding to peak strength, Δ_y is the yield deformation, and α_e is the effective negative post-yield slope given by

$$\alpha_e = \alpha_{P-\Delta} + \lambda(\alpha_2 - \alpha_{P-\Delta}) \tag{9}$$

where α_2 is the negative post-yield slope ratio defined in Figure 6, $\alpha_{P-\Delta}$ is the negative slope ratio caused by $P-\Delta$ effects, and λ is the near-field effect factor given as 0.8 for $S_1 \geq 0.6$ and 0.2 for $S_1 < 0.6$ (S_1 is defined as the 1-second spectral acceleration for the Maximum Considered Earthquake). The α_2 slope includes $P-\Delta$ effects, in-cycle degradation, and cyclic degradation.

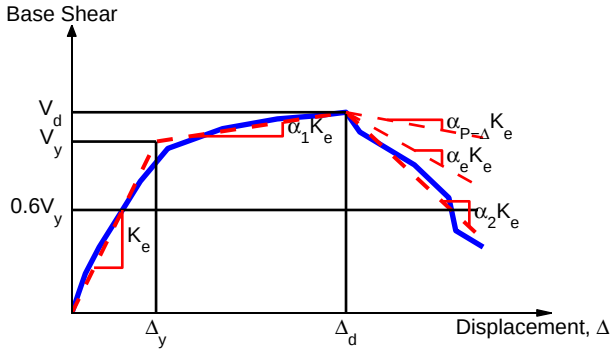

Figure 6. Idealized force-deformation curve in ASCE-41.

FEMA-440 Capacity Spectrum Method

The improved Capacity Spectrum Method presented in FEMA-440 document includes new expressions to determine the effective period and effective damping developed by Guyader and Iwan (2006). Consistent with the original ATC-40 procedure, three iterative procedures for estimating the target displacement are also outlined. Finally, a limitation on the strength is imposed to avoid dynamic instability (Eq. 7).

The improved formulas for effective period and damping ratio in the FEMA-440 document are:

$$T_{eff} = \begin{cases} \left[0.2(\mu-1)^2 - 0.038(\mu-1)^3 + 1\right] T_o; & \mu < 4.0 \\ \left[0.28 + 0.13(\mu-1) + 1\right] T_o; & 4.0 \leq \mu \leq 6.5 \\ \left[0.89\left(\sqrt{\dfrac{(\mu\text{-}1)}{1+0.05(\mu-2)}} - 1\right) + 1\right] T_o; & \mu > 6.5 \end{cases} \quad (10a)$$

$$\zeta_{eff} = \begin{cases} 4.9(\mu-1)^2 - 1.1(\mu-1)^3 + \zeta_o; & \mu < 4.0 \\ 14.0 + 0.32(\mu-1) + \zeta_o; & 4.0 \leq \mu \leq 6.5 \\ 19\left[\dfrac{0.64(\mu-1)-1}{0.64(\mu-1)^2}\right]\left(\dfrac{T_{eq}}{T_o}\right)^2 + \zeta_o; & \mu > 6.5 \end{cases} \quad (10b)$$

These formulas apply for periods in the range of 0.2 and 2.0s. The FEMA-440 document also provides formulas with constants *A* to *L* that are specified depending on the force-deformation relationships (bilinear, stiffness-degrading, strength-degrading) and the post-yield stiffness ratio, α ; these formulas are not included here brevity.

Analytical Model

The three-dimensional analytical models of the selected buildings were developed using the structural analysis software Open System for Earthquakes Engineering Simulation (*OpenSees*) (McKenna and Fenves, 2001). Two models were developed for each building: linearly elastic model for computing the mode shapes and frequencies (or vibration periods), and a nonlinear model for pushover analysis. The beams, columns, and shear walls in the linear elastic model were based on effective section properties recommended in the FEMA-356 document. The size of the rigid-end offset at connection between beam and columns were varied between zero and one times the half the joint size in the appropriate direction. The size of the rigid-end offset was based on matching the computed vibration periods with those identified from recorded motions. The beams, columns, and shear walls were modeled using *elasticBeamColumn* element in *OpenSees*.

The beams, columns, and shear walls in the nonlinear model were modeled either with *beamWithHinges* or *nonlinearBeamColumn* element in *OpenSees*. Both elements used fiber sections containing confined concrete, unconfined concrete, and steel reinforcing bars. The stress-strain behavior of concrete, both confined and confined, was modeled with *Concrete04* material in *OpenSees* (Fig. 7a). This material model, compared to the traditionally used *Concrete01* material model with residual strength (or stress capacity) after crushing strain, enabled capturing of the rapid strength loss after the building's peak strength (see Fig. 6). The crushing strain of the unconfined concrete was selected to be equal to 0.004 and that for confined concrete was selected to be that corresponding to the rupture of confining steel using the well established Mander model. The stress-strain behavior of steel was modeled with *ReinforcingSteel* material in *OpenSees* (Fig. 7b). The strength of concrete and steel was selected based on the values specified in the structural drawings. The P-Delta effects were included in the pushover analysis by applying the gravity loads prior to application of the lateral loads.

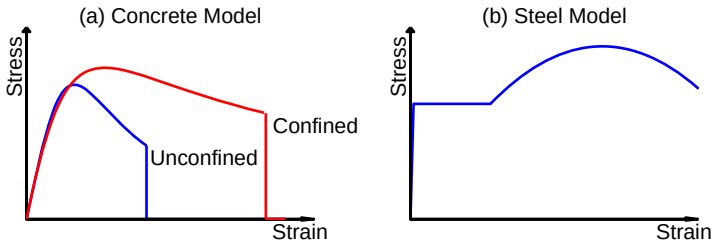

Figure 7. Material models used for nonlinear analysis.

For two of the five selected buildings – 4-Story Commercial Building in Watsonville and 3-Story UCSB Office Building in Santa Barbara – the foundation flexibility was expected to significantly influence the response during strong ground shaking because lateral load resisting system of these two low-rise buildings consists of shear walls in both directions. The foundation

flexibility was included in analytical models of these buildings by attaching six linear springs – three along the x-, y-, and z-translation, two about the x- and y- rocking, and one about the z-torsion – at the base as per the FEMA-356 recommendations.

In addition to all five buildings being modeled in *OpenSees*, a few selected buildings were also modeled using other computer programs: (1) a three dimensional model of the Imperial County Services Building was developed in *CANNY* (Li, 2004); (2) a two dimensional model in the longitudinal direction of the Imperial County Services Building was developed in *CAPP* (Chadwell, 2007); and (3) a two dimensional model in the longitudinal direction of the North Hollywood building was developed in *Peform3D* (CSI, 2006). These models were used to verify the pushover curves from *OpenSees* and investigate the variability in the pushover curves from different analytical programs. This paper presents results from models developed in *OpenSees*; results from models in other programs would be presented in a comprehensive report.

Pushover Curves

Pushover curves for the selected building in the transverse (North-South) and longitudinal (East-West) directions were developed for the fundamental-mode height-wise distribution of lateral loads. These pushover curves are shown in Figs. 8 to 13 with thick solid line along with their idealization, shown in thick dashed line. The idealization is developed from the procedure specified in the FEMA-356 and ASCE-41 documents. Based on the elastic stiffness, K_i, and effective stiffness, K_e, shown as the initial elastic slope of the pushover curve and initial elastic slope of the bilinear idealization, the "effective" period, T_e, was computed from Eq. 2 and is also shown in these figures. Also included is the base-shear strength as a fraction of the total building weight, and the peak roof (or target node) displacement, u_t, recorded during the selected earthquake.

Imperial County Services Building

The pushover curve in the longitudinal direction shows that the Imperial County Services Building begins to rapidly loose strength in the longitudinal direction at roof displacement of about 13 cm (Fig. 8a). This rapid loss of strength is an indication of initiation of failure (or collapse) of the building. The strong-motion data from the 1979 Imperial Valley earthquake indicated a peak roof displacement in the longitudinal direction of 23.58 cm, which far exceeded the displacement capacity of the building in this direction. As a result, the building is expected to collapse during the selected earthquake, an observation which is consistent with the field report (ATC-9, 1984) that this building collapsed primarily due to motions in the longitudinal direction. The pushover curve in the transverse direction, however, does not indicate collapse as the building's displacement capacity exceeded the displacement demand of 5.57 cm (Fig. 8b).

It must be noted that the failure of the building in the longitudinal direction could only be predicted by considering concrete model with crushing in compression. Pushover analysis of analytical models in *OpenSees* or *CANNY*, which did not consider a concrete model with complete loss of strength immediately after crushing, did not predict the building failure prior to the peak roof displacement.

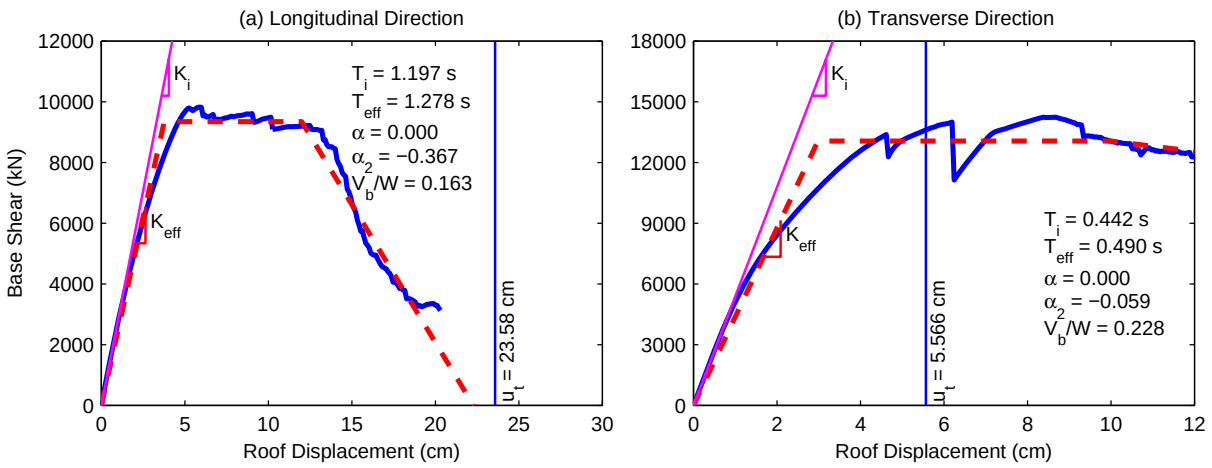

Figure 8. Pushover curves for Imperial County Services Building.

13-Story Commercial Building in Sherman Oaks

The pushover curve of the Sherman Oaks building in the longitudinal direction indicates that the building was deformed beyond the elastic limit during the 1994 Northridge earthquake: the peak roof displacement of 33.6 cm is slightly larger than the effective yield displacement of about 20 cm (Fig 9a). The pushover curve, however, suggests that the building would have collapsed if the roof displacement in the longitudinal direction were to exceed approximately 45 cm due to initiation of rapid loss of strength after this value of roof displacement. The pushover curve in the transverse direction indicates that the building essentially remained elastic in this direction during the 1994 Northridge earthquake as the peak roof displacement is slightly lower than the effective yield displacement (Fig. 9b).

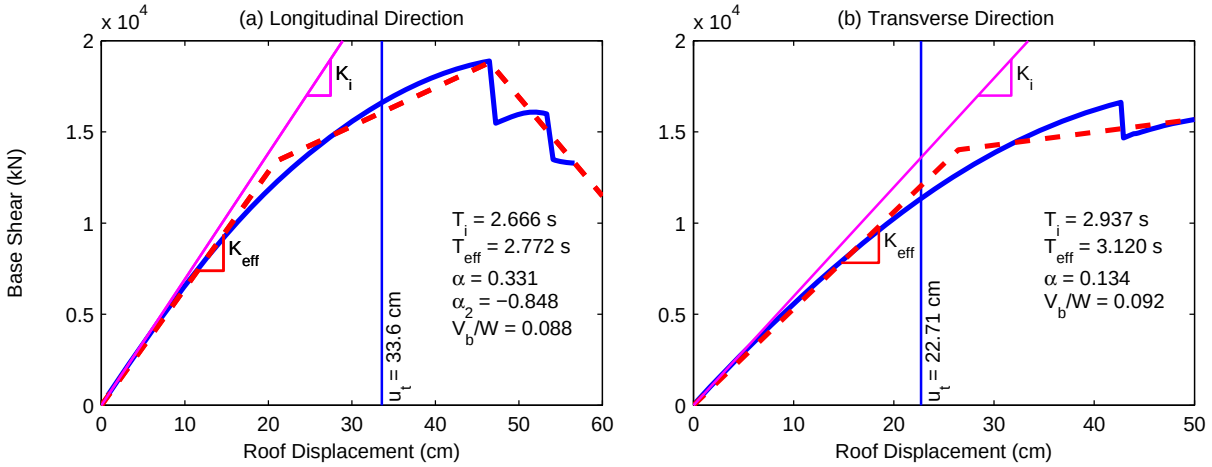

Figure 9. Pushover curves for 13-Story Commercial Building in Sherman Oaks.

In addition to the pushover curves for the entire building (Fig. 9), it is also useful to examine the force-deformation behavior of individual frames. Such results presented in Fig. 10 for the Sherman Oaks building indicate that the strength of interior frame is significantly larger than that of the exterior frame: exterior frame is about 2.5 times stronger in the longitudinal

direction and about 2.0 times stronger in the transverse direction compared to the interior frame. More importantly, the interior frame remains essentially elastic during the 1994 Northridge earthquake, whereas the exterior frame experienced significant nonlinear action.

It must be noted that the Sherman Oaks building suffered significant cracks at many beam-column joints (Shakal et al., 1994). The pushover curves, in particular, in the longitudinal direction clearly indicate the possibility of such damage.

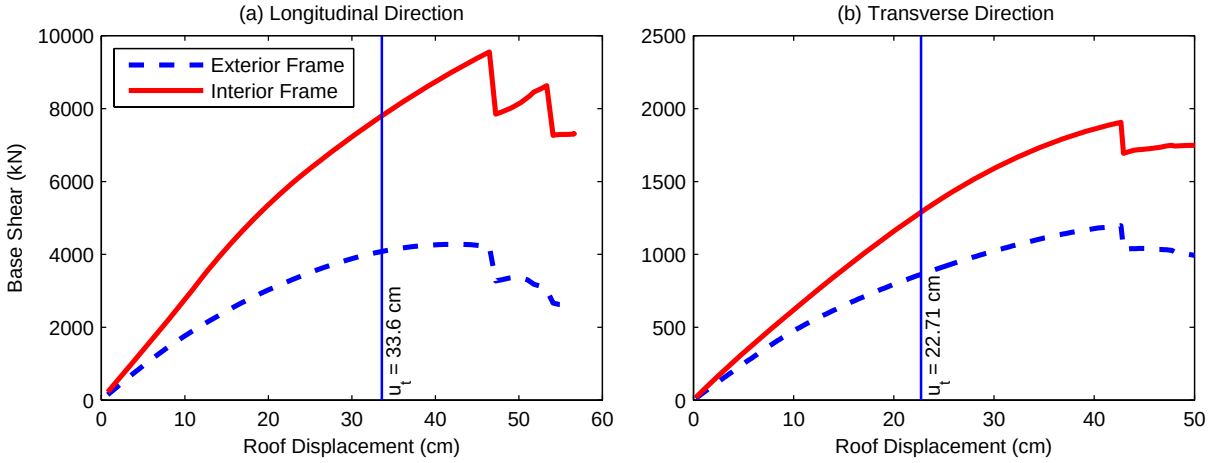

Figure 10. Force-deformation behavior of typical exterior and interior frames of the 13-Story Commercial Building in Sherman Oaks.

20-Story Hotel in North Hollywood

The pushover curves for the North Hollywood Hotel indicate that the building remained well within the linear elastic range both in the longitudinal as well as transverse direction during the 1994 Northridge earthquake (Fig. 11). This building is reported to have suffered heavy nonstructural and content damage but no significant structural damage (Naeim, 1999). The lack of structural damage is consistent with the observations from pushover curves in Fig. 11.

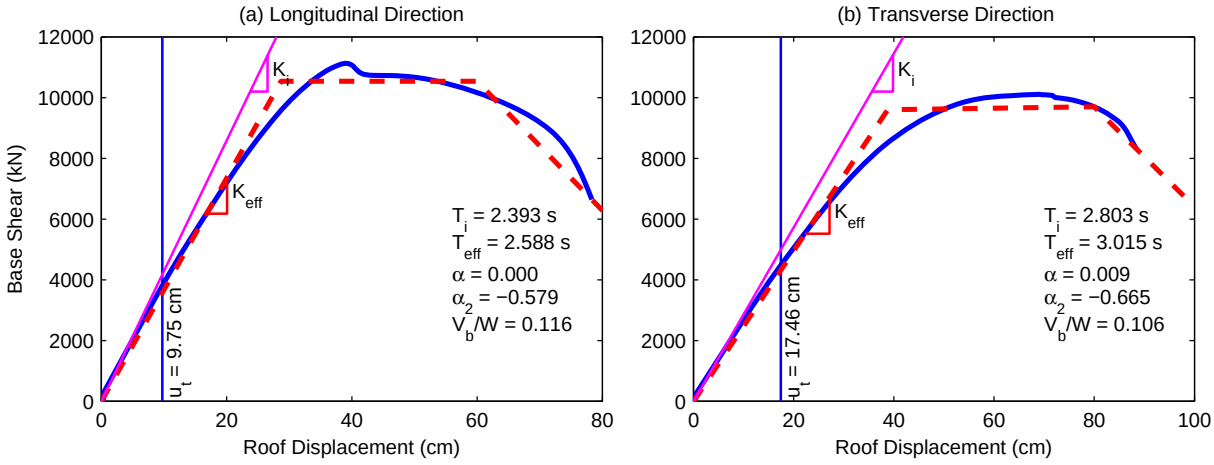

Figure 11. Pushover curves for 20-Story Hotel in North Hollywood.

4-Story Commercial Building in Watsonville

The pushover curves for the Watsonville building indicates that the strength of the building in the longitudinal direction is much lower compared to that in the transverse direction: the building strength is about 0.125W in the longitudinal direction compared to 0.310W in the transverse direction (Fig. 12). Such is the case because the south face of the building has essentially open first story as opposed to shear walls on the remaining three faces. Furthermore, the building was deformed slightly beyond the elastic range in the longitudinal (or East-West) direction but remained essentially elastic in the transverse (or North-South) direction during the 1989 Loma Prieta earthquake.

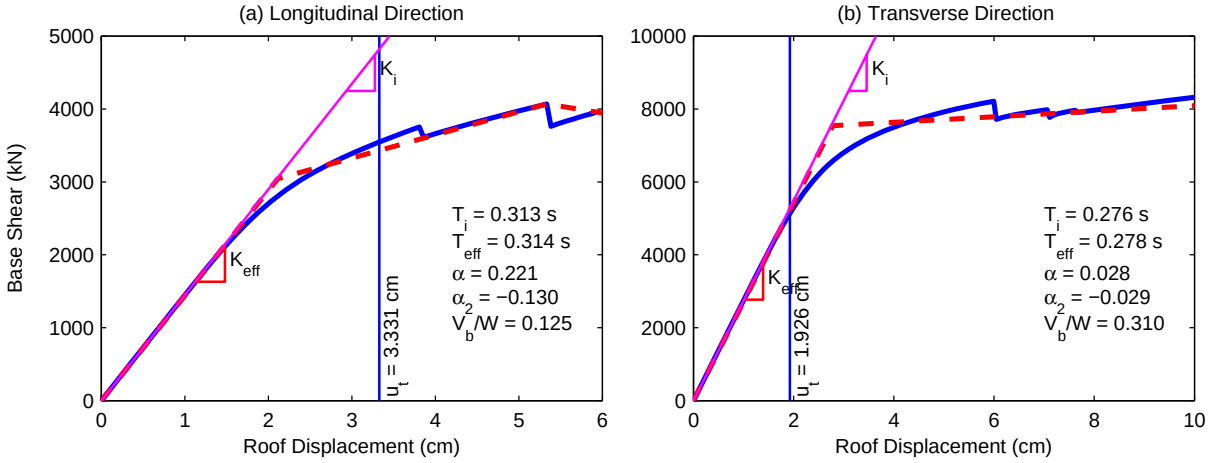

Figure 12. Pushover curves for 4-Story Commercial Building in Watsonville.

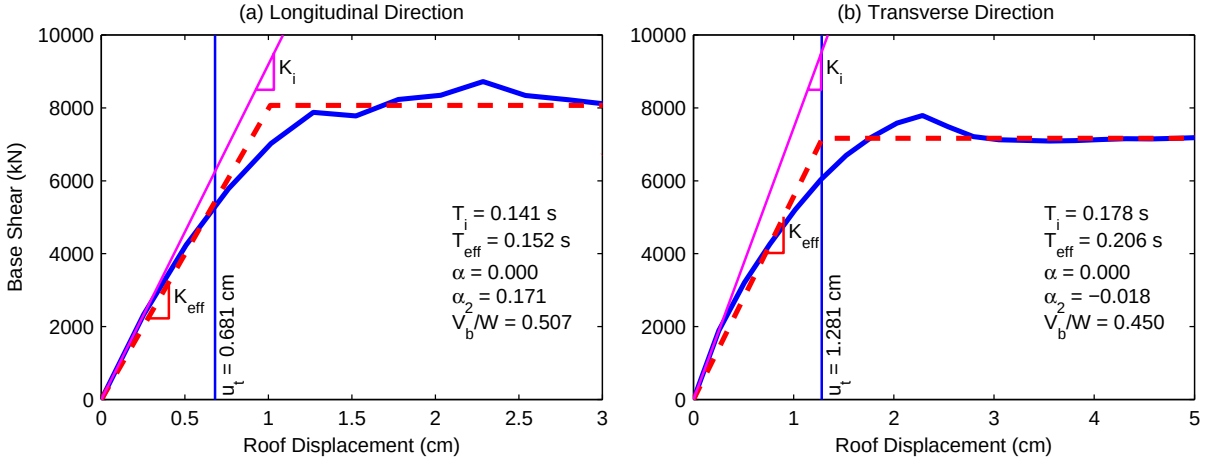

Figure 13. Pushover curves for 3-Story UCSB Office Building in Santa Barbara.

3-Story UCSB Office Building in Santa Barbara

The pushover curves for the Santa Barbara building indicate significant strength of the building compared to what may be expected in typical buildings designed in California: the building strength is 0.507W and 0.450W in the longitudinal and transverse directions,

respectively (Fig. 13). Such higher strengths are due to strengthening of the building with large number of shear walls in both directions in 1975. This building remains well within the linear elastic limit in the longitudinal direction but reaches just about the effective elastic limit in the transverse direction during the1978 Santa Barbara earthquake.

Evaluation of Current NSPs

Current NSPs are evaluated next by comparing the estimates of peak roof (or target node) displacement from the four NSP methods – FEMA-356 CM, ASCE-41 CM, ATC-40 CSM, and FEMA-440 CSM – with the value derived from recorded motions of the selected buildings. The procedure to compute derived roof displacement from recorded motions is available elsewhere (Goel, 2005).

It must be noted that the FEMA-356 CM, ASCE-41 CM, ATC-40 CSM, and FEMA-440 CSM are typically restricted to buildings that respond primarily in the fundamental mode. In this investigation, however, these NSPs were applied to buildings that may have significant contributions form higher modes, e.g., Imperial County Services Building, 13-Story Commercial Building in Sherman oaks, and 20-Story Hotel in North Hollywood. Furthermore, The peak roof displacement in the FEMA-356 and ASCE-41 NSP CM was computed from the 5%-damped elastic response spectrum at vibration period T_e. Similarly, the peak roof displacement is estimated from the damped elastic response spectrum for ζ_{eq} and T_{eq} for the ATC-40 CSM, and for ζ_{eff} and T_{eff} for the FEMA-440 CSM. For each case, the elastic response spectrum is developed for the acceleration recorded at the base of the building in the appropriate direction.

The application of the FEMA-356 CM, ASCE-41 CM, ATC-40 CSM, and FEMA-440 CSM to estimate the peak is illustrated in Figures 14 and 15 for one selected building: 13-Story Commercial Building in Sherman Oaks. The peak roof displacements for all buildings from the various NSP are summarized in Table 2. Errors in the peak roof displacements from various NSP, compared to the peak roof displacements derived from recorded motions, are presented in Fig. 16 with the error defined as

$$E = 100 \times \frac{u_c - u_t}{u_t} \tag{11}$$

in which u_c is the peak roof (or target node) displacement computed form the NSP, and u_t is the corresponding value derived from recorded motions. Note that the peak roof (or target node) displacement derived from recorded motions is considered to be the exact value in computing the error.

The presented results indicate that the roof displacements of the Sherman Oaks building in the longitudinal direction computed from the FEMA-356 and ASCE-41 CM are identical: the roof displacement is 28.04 cm (Figs. 14a and 14b). Such is the case because coefficient C_1 and C_2 in the two NSP are equal to one due to relatively long fundamental vibration period (= 2.67 s) of this building in this direction. This is consistent with the equal-displacement rule, i.e., equal displacements of nonlinear and linear SDF systems, applicable for systems with long vibration

period. The two CSM procedures, however, lead to slightly different values of the roof displacement: ATC-40 CSM gives a value of 24.25 cm (Fig. 14c) and the FEMA-440 CSM provides a value of 27.05 cm (Fig. 14d). The difference between the roof displacements from the two CSM procedures are due to different values of effective period and damping ratio used in these CSM procedures (see Eqs. 5 and 10). Furthermore, the roof displacements from the CM procedures differ from the values from the CSM procedures.

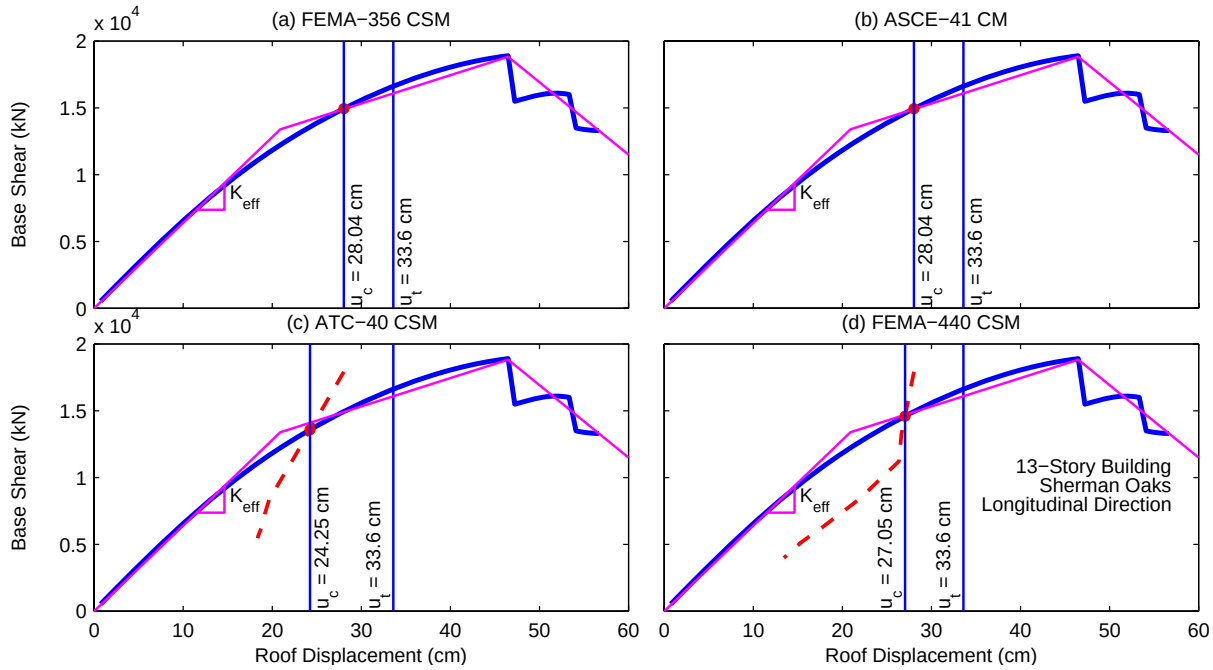

Figure 14. Computation of peak roof displacement in the longitudinal direction of the 13-Story Commercial Building in Sherman Oaks.

All NSP lead to identical peak roof displacement in the transverse direction: the peak roof displacement from various NSP is equal to 17.98 cm (Fig. 15). Such is the case because the building in the transverse direction remains in the linear elastic range. Recall that the coefficients C_1, C_2, and C_3 in the FEMA-356 NSP (Eqs. 3 and 4) as well as the coefficients C_1 and C_2 in the ASCE-41 NSP (Eqs. 6 and 7) are equal to one for a linearly-elastic SDF system, i.e., $R = 1$. Furthermore, the additional terms in the effective vibration period and damping ratio in both the ATC-40 CSM (Eq. 5) and FEMA-440 CSM (Eq. 10) vanish for a linearly-elastic SDF system for $\mu = 1$. Obviously, the target displacement from all NSP would be identical.

The presented results also indicate that the peak roof displacements from NSPs for the Sherman Oaks building are less than those from recorded motions. Such is the case because the NSPs attempt to capture the response only due to the fundamental mode. Such procedures, obviously, can not capture the response due to higher modes; several higher modes contribute to the response of the 13-Story Commercial Building in Sherman Oaks.

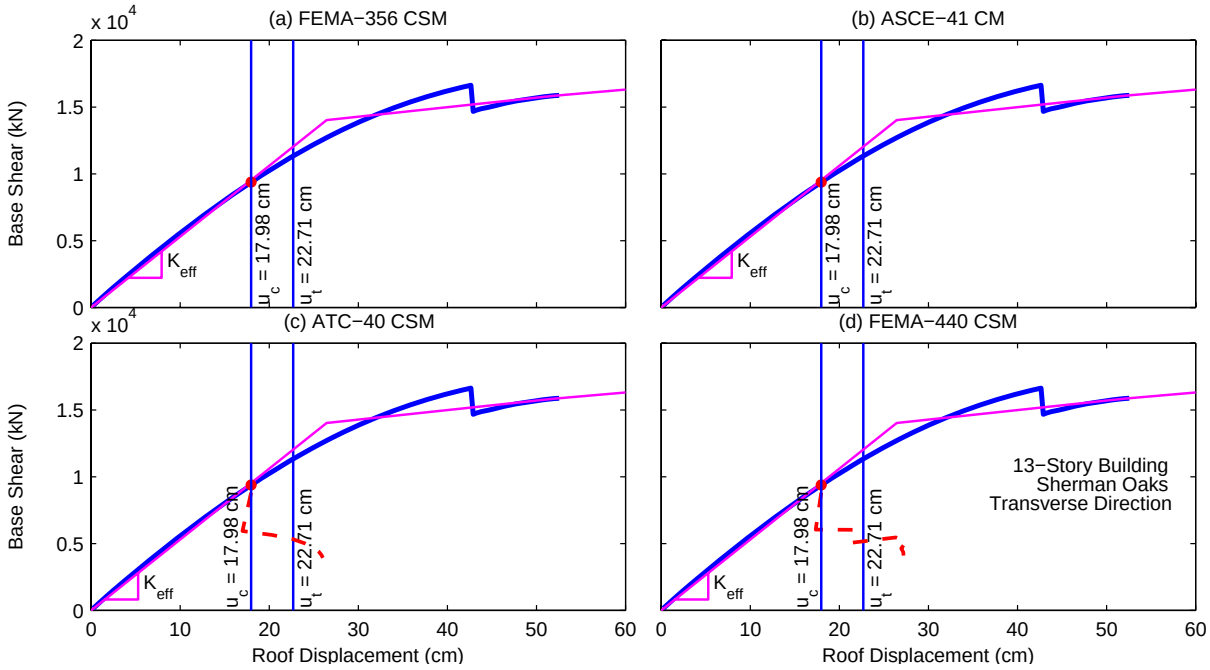

Figure 15. Computation of peak roof displacement in the transverse direction of the 13-Story Commercial Building in Sherman Oaks.

The peak roof displacements estimated from various NSP, along with the value derived from recorded motions, are summarized in Table 2. Note that peak roof displacements for the Imperial County Services Building and the Watsonville Commercial Building in the longitudinal direction could not be computed from various NSP and hence are denoted as not available (N/A).

Table 2. Peak roof displacements from various NSP.

Peak Roof Displacement (cm)					
	Rec.	**FEMA-356 CM**	**ASCE-41 CM**	**ATC-40 CSM**	**FEMA-440 CSM**
Imperial County Services Building (IC)					
Longitudinal (EW)	23.58	N/A	N/A	N/A	N/A
Transverse (NS)	5.57	6.99	7.60	5.64	5.46
Sherman Oaks Commercial Building (SO)					
Longitudinal (EW)	33.60	28.04	28.04	24.25	27.05
Transverse (NS)	22.71	17.98	17.98	17.98	17.98
North Hollywood Hotel (NH)					
Longitudinal (EW)	9.75	10.17	10.17	10.17	10.17
Transverse (NS)	17.46	14.33	14.33	14.33	14.33
Watsonville Commercial Building (WT)					
Longitudinal (EW)	3.33	N/A	N/A	N/A	N/A
Transverse (NS)	1.93	1.66	1.56	2.58	2.61
Santa Barbara Office Building (SB)					
Longitudinal (EW)	0.68	0.45	0.38	0.67	0.67
Transverse (NS)	1.28	1.08	0.93	1.06	1.19

It is expected that the various NSPs, which primarily should differ only for buildings responding in the nonlinear range, should provide identical values of peak roof displacements. While this expectation is confirmed for the Sherman Oaks Commercial Building in the transverse direction and the North Hollywood Building in both directions, such is not the case for the Watsonville Commercial Building in the transverse direction and the Santa Barbara Office Building in both directions (Table 2). Recall that these buildings (in indicated directions) did not deformed beyond the linear elastic range during the selected earthquake; see pushover curves for Sherman Oaks Building in the transverse direction (Fig. 9b), North Hollywood Hotel in both directions (Figs. 11a and 11b), Watsonville Commercial Building in the transverse direction (Fig. 12b), and Santa Barbara Office Building in both directions (Figs. 13a and 13b). The primary difference between these buildings is the length of the fundamental vibration period: the taller Sherman Oaks Commercial Building and the North Hollywood Building have fundamental vibration periods that exceed 2.0 s whereas the shorter Watsonville Commercial Building and the Santa Barbara Office Building have fundamental vibration periods that are less than 0.5 s. Therefore, the presented results indicate that the various NSP provide identical estimates of peak roof displacement for a long-period, linearly-elastic building but may lead to different estimates for a short-period, linearly-elastic building.

The aforementioned discrepancy in roof displacement from various NSPs for short-period, linearly-elastic buildings occurs due to high sensitivity of the R value in the CM procedures and the μ value in the CSM procedure to even very small errors in estimating the period and damping ratio. It is well known that the linearly-elastic response spectrum tends to be very jagged in the short-period range. As a result, estimates of the peak response of the linearly-elastic SDF system tends to be sensitive to errors in the vibration period and damping ratio. For the FEMA-356 CM and ASCE-41 CM, even the slight errors in estimating the vibration period and damping ratio may lead to the value of R needed in estimating the various coefficients (see Eqs. 3, 4, 6, and 7) to be larger than one. For similar reasons, the μ needed in the ATC-40 CSM and FEMA-440 CSM to compute the effective period and effective damping ratio (see Eqs. 5 and 10) may become larger than one. Recall that for linearly-elastic buildings, values of both R and μ should be equal to one. Depending on by how much the R and μ values differ from one, the various NSPs would obviously lead to different values of the peak roof displacement for short-period, linearly-elastic buildings. Since the linearly-elastic response spectrum in the long-period range tends to be smooth, errors in vibration period and damping ratio do not affect the peak roof displacement estimate, and hence the R and μ values, of the long-period, linearly elastic systems.

The FEMA-356 CM and ASCE-41 CM provide identical values of the peak roof displacements for the two flexible buildings – Sherman Oaks Commercial Building and the North Hollywood Building. As noted previously, this occurs because the coefficients C_1 and C_2 for these buildings are identical in the two NSP due to fundamental vibration periods being longer than 1 s. For the remaining three stiff buildings – Imperial County services Building (transverse direction only), Watsonville Commercial Building and Santa Barbara Office Building – however the two NSP lead to different estimates of peak roof displacements as the coefficients C_1 and C_2 differ between the two NSP for short-period buildings.

Figure 16 presents the percent error (see Eq. 11) in the peak roof displacement from various NSPs when compared to the value derived from recorded motions. These results indicate significant errors in the estimate of peak roof displacement from current NSPs. These errors range from about 40% underestimation, e.g., as is the case for ASCE-41 CM for the Santa Barbara building (see SB-EW in Fig. 16), to about 40% overestimation, e.g., FEMA-440 iterative CSM for the Watsonville building (see WT-NS in Fig 16) .

Among the two CM procedures, the ASCE-41 CM, which is based on the improvements suggested recently in the FEMA-440 document, does not necessarily provide improved estimates for the selected buildings. For example, the ASCE-41 CM leads to larger overestimation for the Imperial County Services Building (see IC-NS in Fig. 16) and larger underestimation for Watsonville and Santa Barbara buildings (see WT-NS, SB-EW, and SB-NS in Fig. 16) when compared to the results from the FEMA-356 CM.

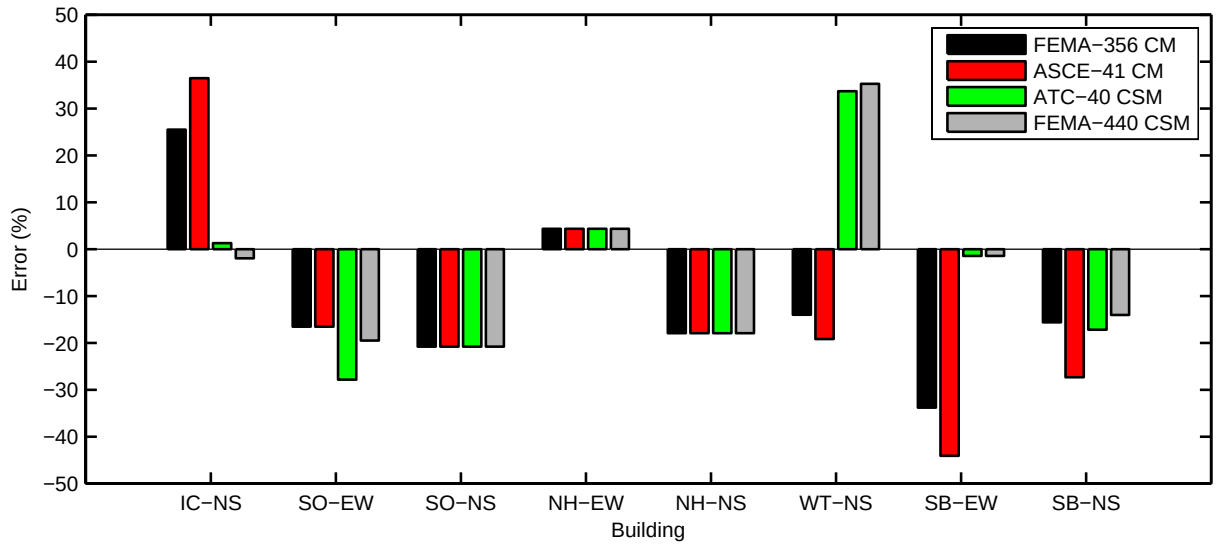

Figure 16. Percent error in peak roof displacements from various NSPs.

The FEMA-440 CSM generally provides better estimated of the peak roof displacement compared to the ATC-40 CSM (see IC-NS, SO-EW, and SB-NS in Fig. 16). This indicates that the improvements to the CSM procedure suggested in the FEMA-440 document are likely to lead to better estimated of peak roof displacement.

Finally, there is no clear evidence of whether the CM procedure (FEMA-356 or ASCE-41) or the CSM procedure (ATC-40 or FEMA-440) provides better estimate of peak roof displacement when compared with the value derived from recorded motions. The CSM procedure lead to better estimates for some building (see IC-NS and SB-EW in Fig. 16) but worse estimates for other (see SO-EW and WT-NS in Fig. 16) compared to the CM procedure. For other buildings, the two procedures lead to essentially similar level of accuracy (see SO-NS, NH-EW, and NH-NS in Fig. 16).

Conclusions

This investigation on evaluation of the FEMA-356 CM, ASCE-41 CM, ATC-40 CSM, and FEMA-440 CSM using strong-motion records of five reinforced-concrete building have led to the following conclusions:

1. The pushover curve for the entire building that is used in implementation of the NSP may not truly reveal the extent of nonlinearity in the building during an earthquake. This may occur for buildings in which strength and stiffness properties of lateral-load resisting elements (such as frames, walls) differ significantly.

2. The various NSPs may lead to either significant overestimation or underestimation of the peak roof displacement.

3. It is expected that various NSPs provide identical estimates of peak roof displacement for buildings responding in the linearly-elastic range during an earthquake. While this expectation is found to be valid for flexible (long-period) buildings, it may not be valid for stiff (short-period) buildings.

4. The ASCE-41 CM, which is based on recent improvements to the FEMA-356 CM suggested in FEMA-440 document, does not necessarily provide better estimate of roof displacement for the buildings considered in this investigation.

5. The improved FEMA-440 CSM generally provides better estimates of peak roof displacements compared to the ATC-40 CSM.

6. There is no conclusive evidence that the CM procedures (FEMA-356 or ASCE-41) lead to better estimates of the peak roof displacement compared to the CSM procedure (ATC-40 or FEMA-440) or vice-versa.

It must be emphasized that the NSPs are typically designed to be used with smooth spectrum. Ideally, these procedures must be evaluated using a suite of design spectrum compatible ground motions, a wide range of buildings, and statistical analysis of results. Although, the evaluation of various NSPs in this investigation is conducted based on limited data – five buildings and one set of strong motion records for each building – and this investigation has led to some useful observations, it is still not possible to draw definitive conclusions about all aspects of various NSPs. More definitive conclusions may be drawn as additional data becomes available in future.

Acknowledgment

This investigation is supported by the California Department of Conservation, California Geological Survey, Strong Motion Instrumentation Program, Contract No. 1005-832. This support is gratefully acknowledged. Also acknowledged is the contribution to this research investigation by Matthew Hazen and Joey Givens, undergraduate students at Cal Poly, San Luis Obispo, and by Dr. Dae-Han Jun, Visiting Professor from Dongseo University, Korea.

References

ASCE (2000). Prestandard and Commentary for the Seismic Rehabilitation of Buildings. *Report No. FEMA-356*, Building Seismic Safety Council, Federal Emergency Management Agency, Washington, D.C.

Aschheim, M. A., Maffei, J. and Black, E. (1998). "Nonlinear Static Procedures and Earthquake Displacement Demands." *Proceedings of 6th U.S. National Conference on Earthquake Engineering*, Earthquake Engineering Research Institute, Seattle, WA.

Akkar, S. and Metin, A. (2007). "Assessment of Improved Nonlinear Static Procedures in FEMA-440." *Journal of Structural Engineering*, **133**(9): 1237-1246.

ATC-40 (1997). Seismic Evaluation and Retrofit of Concrete Buildings. *Report No. ATC-40*, Applied Technology Council, Redwood City, CA.

ATC-55 (2003). Improvement of Inelastic Seismic Analysis Procedures: Draft Report for Atc-55 Project. *Report No. FEMA-440*, Applied Technology Council, Redwood City, CA.

ATC-9 (1984). An Evaluation of the Imperial County Services Building: Earthquake Response and Associated Damage. *Report No. ATC-9*, Applied Technology Council, Palo Alto, CA.

Chadwell, C. (2007). Capacity Analysis and Pushover Program (Capp): Version 1.04. Imbsen & Associates, Inc., (www.imbsen.com).

Chopra, A. K. and Goel, R. K. (2000). "Evaluation of NSP to Estimate Seismic Deformation: SDF Systems." *Journal of Structural Engineering*, **126**(4): 482-490.

CSI (2006). Perform3D: Nonlinear Analysis and Performance Assessment for 3d Structures: Version 4. Computers and Structures, Inc., Berkeley. (www.csiberkeley.com).

Goel, R. K. (2005). "Evaluation of Modal and FEMA Pushover Procedures Using Strong-Motion Records of Buildings." *Earthquake Spectra*, **21**(3): 653-684.

Goel, R.K. (2007). "Evaluation of Current Nonlinear Static Procedures Using Strong Motion Records," *Proceedings of the 2007 Structures Congress, Long Beach, CA*, American Society of Civil Engineers, Reston, VA.

Guyader, A. C. and Iwan, W. D. (2006). "Determining Equivalent Linear Parameters for Use in a Capacity Spectrum Method." *Journal of Structural Engineering*, **132**(1): 59-67.

Li, K. (2004). CANNY: 3-Dimensional Nonlinear Static/Dynamic Structural Analysis Computer Program: CANNY Consultant PTE LTD, Singapore.

McKenna, F. and Fenves, G. (2001). The Opensees Command Language Manual: 1.2. Pacific Earthquake Engineering Center, University of California, Berkeley,(http://opensees.berkeley.edu).

Miranda, E. and Ruiz-Garcia, J. (2002). "Evaluation of Approximate Methods to Estimate Maximum Inelastic Displacement Demands." *Earthquake Engineering and Structural Dynamics*, **31**(3): 539-560.

Naeim, F. (1999). "Lessons Learned from Performance of Nonstructural Components During the January 17, 1994 Northridge Earthquake -- Case Studies of Six Instrumented Multistory Buildings." *Journal of Seismology and Earthquake Engineering*, **2**(1): 47-57.

Shakal, A. F., Huang, M. and Darragh, R. B. (1994). “Some Implications of Strong-Motion Records from the 1994 Northridge Earthquake.” *Proceedings of SMIP94 Seminar on Utilization of Strong-Motion Data*, Strong Motion Instrumentation Program, CDMG, Sacramento, CA.